

Contents lists available at ScienceDirect

Nuclear Engineering and Technologyjournal homepage: www.elsevier.com/locate/net**Original Article****A frame work for heat generation/absorption and modified homogeneous–heterogeneous reaction in flow based on non-Darcy–Forchheimer medium**

Tasawar Hayat ^{a, b}, Salman Ahmad ^a, Muhammad I. Khan ^{a, **}, Muhammad I. Khan ^{c, *}, Ahmed Alsaedi

^a Department of Mathematics, Quaid-I-Azam University 45320, Islamabad 44000, Pakistan

^b NAAM Research Group, Department of Mathematics, Faculty of Science, King Abdulaziz University 21589, Jeddah 21589, Saudi Arabia

^c Heriot Watt University, Edinburgh Campus, Edinburgh EH14 4AS, Faculty of Engineering, United Kingdom

ARTICLE INFO**Article history:**

Received 7 June 2017

Received in revised form

1 January 2018

Accepted 8 January 2018

Available online 2 March 2018

Keywords:

Cross Fluid

Heat Generation/Absorption

Homogeneous–Heterogeneous Reactions

Non-Darcy–Forchheimer Medium

Thermal Radiation

ABSTRACT

The present work aims to report the consequences of Darcy–Forchheimer medium in flow of Cross fluid model toward a stretched surface. Flow in porous space is categorized by Darcy–Forchheimer medium. Further heat transfer characteristics are examined via thermal radiation and heat generation/absorption. Transformation procedure is used. The arising system of nonlinear ordinary differential equations is solved numerically by means of shooting method. The effects of different flow variables on velocity, temperature, concentration, skin friction, and heat transfer rate are discussed. The obtained outcomes show that velocity was enhanced with the increase in the Weissenberg number but decays with increase in the porosity parameter and Hartman number. Temperature field is boosted by thermal radiation and heat generation; however, it decays with the increase in the Prandtl number.

© 2018 Korean Nuclear Society, Published by Elsevier Korea LLC. This is an open access article under the CC BY-NC-ND license (<http://creativecommons.org/licenses/by-nc-nd/4.0/>).

1. Introduction

In nature, there are different fluids, including hydrogenated castor oil, drilling mud, jam, synovial fluids, mayonnaise, butter, ketchup, shampoos, soup, gypsum paste, cheese, printer ink, toothpaste taffy, yogurt, clays, paints, colloidal suspension, blood, etc., that do not satisfy Newton's law of viscosity. Such fluids are referred to as non-Newtonian fluids. Non-Newtonian fluids cannot be handled through single Navier–Stokes relations. But there are various engineering and industrial applications of non-Newtonian fluids. Therefore, many researchers and scientists have developed different models, such as the Maxwell, Williamson, second grade, third grade, Sutterby, Cross, Casson, Oldroyd-B, Burgers, micro-polar, generalized Burgers, Sisko, Jeffrey, etc., for non-Newtonian fluids. Some studies about non-Newtonian fluids can be found in the references [1–6].

Chemical reaction and thermal radiation influences on mass and heat transfer over an extended surface have vital importance in engineering and physics because of the various applications of materials, such as combustion of fossil fuels, nuclear power flows, fuel turbines, liquids, steel fluid, plasma, picture ionization, wind tunnels, geophysics, and a wide variety of propulsion devices for planes, satellites, and aerial motors. The effects of nonlinear thermal radiation and induced magnetic field on flow of viscoelastic liquid with heterogeneous–homogeneous reactions are explored by Animasaun et al. [7]. Qayyum et al. [8] analyzed the influence of homogeneous–heterogeneous reactions in flow based on copper and silver water nanoparticles. Khan et al. [9] point out the significance of mixed convection of Walter-B nanofluid with thermal radiation. For further studies about thermal radiation and chemical reactions, refer to the references [10–20].

The study of flow through porous medium has wide range applications in different fields, including petroleum engineering and geothermal operations. Characterization of flow through a porous medium is known to depend on a dimensionless number (the Reynolds number). For low flow rates (i.e., $Re < 1$, which means that pressure gradient and flow rate are linearly related), Darcy's law is valid. This law states that viscous forces are greater than inertial

* Corresponding author.

** Corresponding author.

E-mail addresses: mikhan@math.qau.edu.pk (M.I. Khan), mk42@hw.ac.uk (M.I. Khan).

forces in a porous medium. Commonly, flow in a porous medium is analyzed using Darcy's law, but this law is not sufficient for high flow rates. For higher velocity flow, the Forchheimer formula is used. Forchheimer [21] proposed a new nonlinear relation for higher flow rates. Hayat et al. [22] explored non-Darcy–Forchheimer flow of second grade ferromagnetic liquid past a stretchable surface. Several investigations related to non-Darcy–Forchheimer flow are discussed in the references [23,24].

Our main focus here is to investigate the flow of a cross fluid in a porous medium. The porous medium is characterized by the non-Darcy–Forchheimer relation. Moreover, the impacts of chemical reaction, magnetohydrodynamics (MHD), heat generation, and thermal radiation are also accounted. The governing partial differential equations are transformed into ordinary differential equations through appropriate transformation. Numerically, the system of the ODEs is tackled using the Built-in-Shooting technique [25–28]. Characteristics of velocity, temperature, concentration, skin friction, and Nusselt number with variation of flow variable are analyzed.

2. Materials and methods

Here, steady, incompressible two-dimensional flow of a cross fluid in a porous medium is considered. Fluid is made electrically conducting by the application of a magnetic field. Induced magnetic field is ignored due to small Reynolds number. Further heat transport characteristics are discussed in the presence of thermal radiation and heat source/sink. Homogeneous–heterogeneous reactions are also considered. The flow configuration is presented in Fig. 1.

The porous medium is analyzed by Forchheimer relation. The relation for the heterogeneous–homogeneous reaction is taken as follows [25]:

$$A + 2B \rightarrow 3B, \quad \text{rate} = k_1 C_a C_b^2, \quad (1)$$

$$A + B \rightarrow 3B, \quad \text{rate} = k_2 C_a. \quad (2)$$

Here, k_1 and k_2 indicate the reaction rates, and C_a and C_b are the concentrations of chemical species A and B , respectively. The considered boundary layer flow expressions are [1,6]

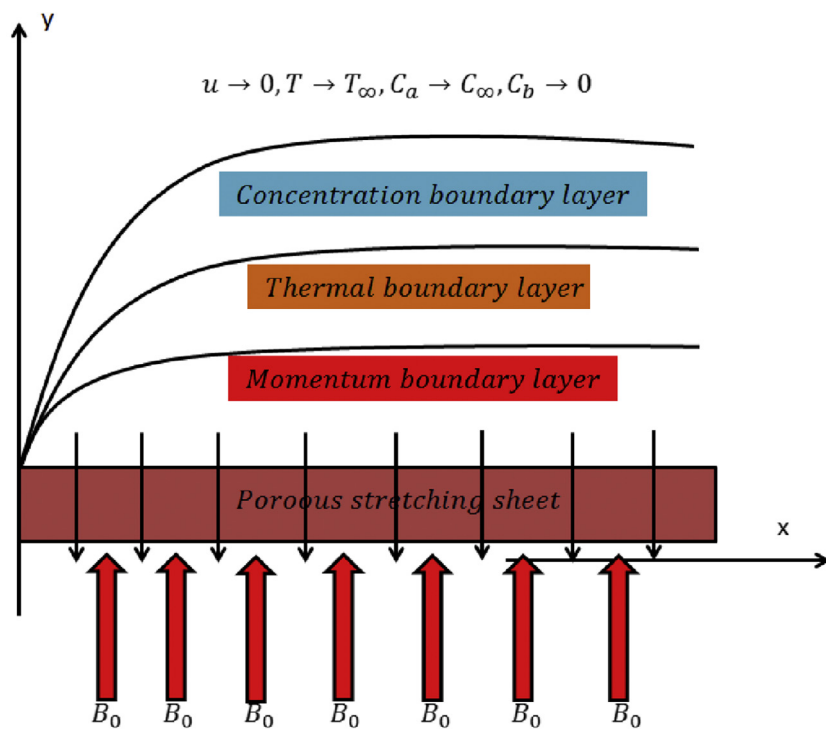
$$\frac{\partial u}{\partial x} + \frac{\partial v}{\partial y} = 0, \quad (3)$$

$$u \frac{\partial u}{\partial x} + v \frac{\partial u}{\partial y} = v \frac{\partial}{\partial y} \left[\frac{\frac{\partial u}{\partial y}}{1 + \left\{ \Gamma \left(\frac{\partial u}{\partial y} \right) \right\}^n} \right] - \frac{\sigma}{\rho} B_0^2 u - \frac{\nu \phi}{K^*} u - \frac{c_b \phi}{\sqrt{K^*}} u^2, \quad (4)$$

$$\rho c_p \left(u \frac{\partial T}{\partial x} + v \frac{\partial T}{\partial y} \right) = k \frac{\partial^2 T}{\partial y^2} + \frac{16 \sigma^* T_\infty^3}{3k^*} \frac{\partial^2 T}{\partial y^2} + Q_0 (T - T_\infty) - \left(\frac{\Delta H_s}{\delta_A} \right) (k_1 C_a C_b^2), \quad (5)$$

$$u \frac{\partial C_a}{\partial x} + v \frac{\partial C_a}{\partial y} = D_A \frac{\partial^2 C_a}{\partial y^2} - k_1 C_a C_b^2, \quad (6)$$

$$u \frac{\partial C_b}{\partial x} + v \frac{\partial C_b}{\partial y} = D_B \frac{\partial^2 C_b}{\partial y^2} + k_1 C_a C_b^2, \quad (7)$$



$$u = u_w = cx, \quad v = 0, \quad -k \frac{\partial T}{\partial y} = k_2 C_a \left(\frac{-\Delta H_s}{\delta_A} \right), \quad D_A \frac{\partial C_a}{\partial y} = k_2 C_a, \quad D_B \frac{\partial C_b}{\partial y} = -k_s C_a$$

Fig. 1. Systematic diagram of the flow analysis.

$$\left. \begin{aligned} u = u_w = cx, v = 0, -k \frac{\partial T}{\partial y} = k_2 C_a \left(-\frac{\Delta H_s}{\delta_A} \right), \\ D_A \frac{\partial C_a}{\partial y} = k_s C_a, D_B \frac{\partial C_a}{\partial y} = -k_s C_a \text{ at } y = 0, \\ u \rightarrow 0, T \rightarrow T_\infty, C_a \rightarrow C_\infty, C_b \rightarrow 0 \text{ when } y \rightarrow \infty. \end{aligned} \right\} \quad (8)$$

Here, u and v denote velocity components, ν kinematic viscosity, ρ density, n power law index, Γ material time constant, σ electric conductivity, B_0 magnetic field strength, ϕ porosity parameter, K^* specific or intrinsic permeability, c_p specific heat, k thermal conductivity, T temperature, σ^* Stefan–Boltzman constant, k^* mean absorption coefficient, T_∞ ambient temperature, Q_0 heat generation/absorption coefficient, D_A and D_B diffusion coefficients, k_s heat transfer coefficient, and c stretching rate.

Considering

$$\left. \begin{aligned} \psi = \sqrt{c\nu x}f(\eta), u = \frac{\partial \psi}{\partial y} = cx f'(\eta), v = -\frac{\partial \psi}{\partial x} = -\sqrt{c\nu}f(\eta), \eta = \sqrt{\frac{c}{\nu}}y, \\ \theta(\eta) = \frac{T - T_\infty}{T_w - T_\infty}, g(\eta) = \frac{C_a}{C_\infty}, h(\eta) = \frac{C_b}{C_\infty}. \end{aligned} \right\} \quad (9)$$

Eq. (3) is trivially fulfilled, and the remaining Eqs. (4–8) become

$$\left[1 + (1 - n) \left(Wef'' \right)^n \right] f''' - \left[1 + \left(Wef'' \right)^n \right]^2 [f'^2 - ff'' + Ha f' + \beta f' + \beta_0 f'^2] = 0, \quad (10)$$

$$(1 + Tr)\theta'' + Pr(f\theta' + \lambda\theta) + \gamma gh^2 = 0, \quad (11)$$

$$g'' - ScKgh^2 + Scfg' = 0, \quad (12)$$

$$h'' + ScKgh^2 + Sch'f = 0, \quad (13)$$

$$\left. \begin{aligned} f(0) = 0, f'(0) = 1, \theta'(0) = K_T g(0), g'(0) = K_s g(0), h'(0) = -\frac{K_s}{\delta} g(0), \\ f'(\infty) \rightarrow 0, \theta(\infty) = 0, g(\infty) = 1, h(\infty) = 0. \end{aligned} \right\} \quad (14)$$

In the above expressions, $We (= c\Gamma Re_x^{1/2})$ indicates Weissenberg number, $Ha (= \frac{\sigma B_0^2}{\rho c})$ Hartmann number, $\beta (= \frac{\nu\phi}{cK^*})$ Darcy porosity parameter, $\beta_0 (= \frac{c_p\phi}{\sqrt{K^*}} \sqrt{\frac{\nu}{c}} Re_x^{1/2})$ local inertia coefficient parameter, $Tr (= \frac{16\sigma^* T_\infty^3}{3kk^*})$ thermal radiation parameter, $Pr (= \frac{\mu_0 c_p}{k})$ Prandtl number, $\lambda (= \frac{Q_0}{c\rho c_p})$ heat generation/absorption parameter, $Sc (= \frac{\nu}{D_h})$ Schmidt number, $\gamma (= k_1 \frac{\Delta H_s}{\rho c_p \delta_A} \frac{C_\infty^3}{c(T - T_\infty)})$ homogeneous reaction heat parameter, $\delta (= \frac{D_B}{D_A})$ ratio of diffusion rate, $K (= \frac{k_1 c_\infty^2}{c})$ homogeneous variable, $K_T (= \frac{k_2}{k} \frac{C_\infty}{(T_w - T_h)} \frac{\Delta H_s}{\delta_A} \sqrt{\frac{\nu}{c}})$ thermal conductivity with respect to homogeneous reaction, and $K_s (= \frac{k_s}{D_A} \sqrt{\frac{\nu}{c}})$ heterogeneous parameter. Taking the case in which the mass diffusion coefficients are equal, i.e., $\delta = 1$:

$$h(\eta) + g(\eta) = 1. \quad (15)$$

Using Eq. (15), Eqs. (11–13) become

$$(1 + Tr)\theta'' + Pr(f\theta' + \lambda\theta) + \gamma g(1 - g)^2 = 0, \quad (16)$$

$$g'' - ScKg(1 - g)^2 + Scfg' = 0, \quad (17)$$

3. Quantities of curiosity

Mathematical expressions of velocity and temperature gradients are

$$C_{fx} = \frac{-2\tau_w}{\rho u_w^2}, \quad Nu_x = \frac{xq_w}{k(T_w - T_\infty)}, \quad (18)$$

where

$$\left. \begin{aligned} \tau_w = (\tau_{yx})_{y=0} = \left[\mu_0 \frac{\frac{\partial u}{\partial y}}{1 + \left(\Gamma \frac{\partial u}{\partial y} \right)^n} \right], \\ q_w = -k \left[1 + \frac{16\sigma^* T_\infty^3}{3kk^*} \right] \left[\frac{\partial T}{\partial y} \right]_{y=0}. \end{aligned} \right\} \quad (19)$$

Invoking Eq. (19) in Eq. (18), one obtains

$$C_{fx} Re_x^{0.5} = \frac{-2f''(0)}{1 + (Wef''(0))^n}, \quad Nu_x Re_x^{-0.5} = -(1 + Tr)\theta'(0), \quad (20)$$

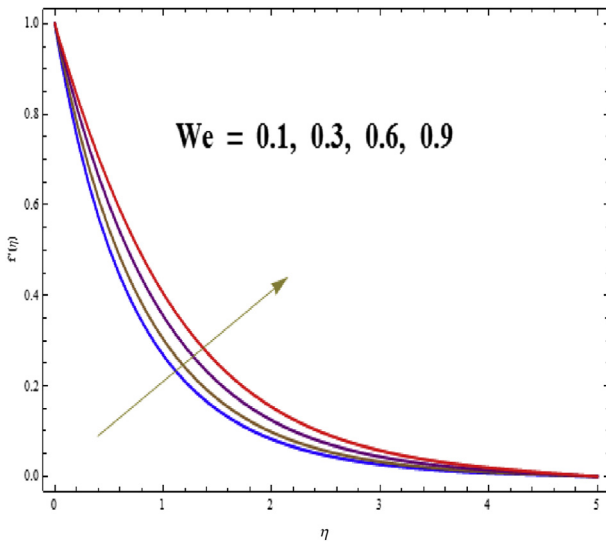
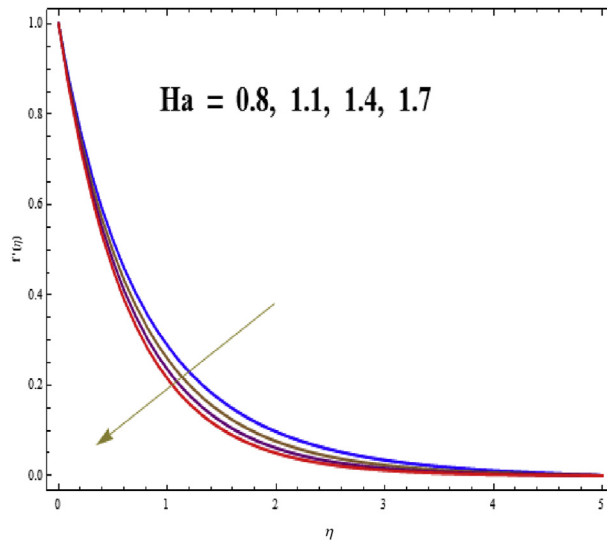
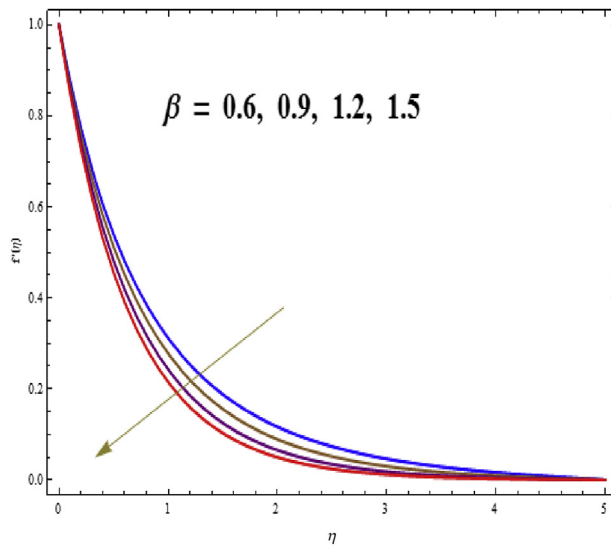
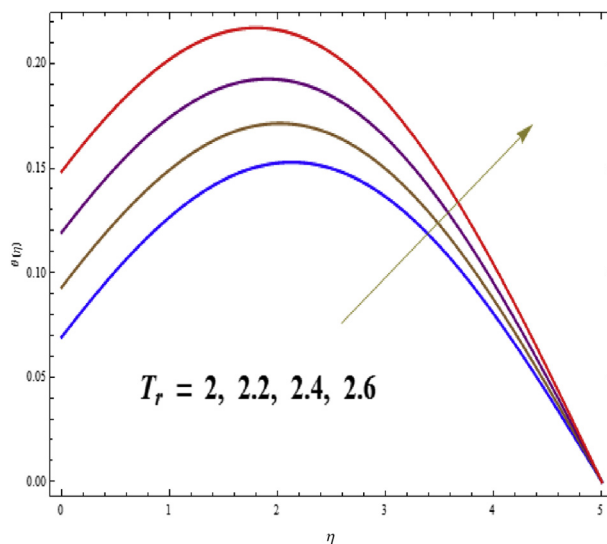
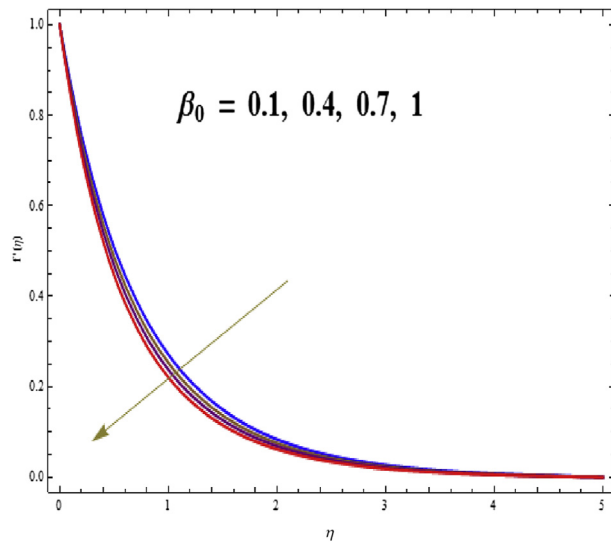
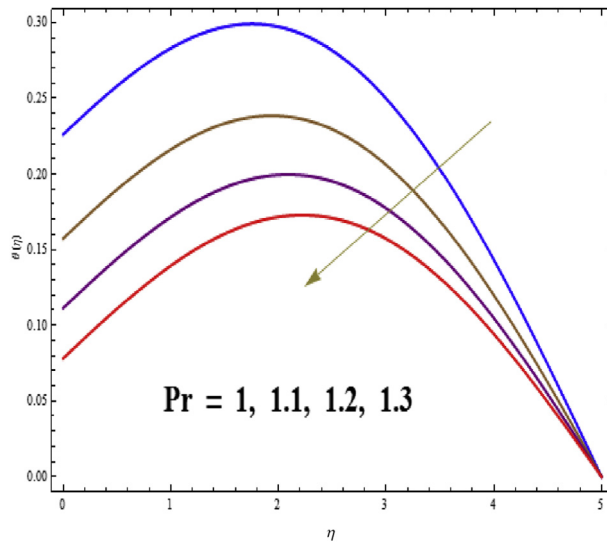
where $Re_x (= \frac{cx^2}{\nu})$ the local Reynolds number.

4. Results and discussion

In this portion, we aim to numerically obtain the nonlinear ordinary system of differential equations with the help of the numerical method, the Built-in-Shooting technique. Here, we analyze the impacts of various flow variables on velocity ($f'(\eta)$), temperature ($\theta(\eta)$), and concentration ($g(\eta)$). Attention is particularly given to variables Weissenberg number (We), Hartmann number (Ha), Darcy porosity parameter (β), local inertia coefficient parameter (β_0), thermal radiation parameter (Tr), Prandtl number (Pr), heat generation/absorption parameter (λ), Schmidt number (Sc), homogeneous reaction heat parameter (γ), ratio of diffusion rate (δ), homogeneous variable (K), thermal conductivity with respect to homogeneous reaction (K_T), and heterogeneous parameter (K_s).

Figs. 2–5 are plotted to describe the influence of Weissenberg number (We), Hartmann number (Ha), Darcy porosity parameter (β), and local inertia coefficient parameter (β_0) on velocity ($f'(\eta)$). The effect of (We) on ($f'(\eta)$) is portrayed in Fig. 2. It should be noted that velocity was enhanced for larger estimation of (We). This is because (We) is an increasing function of the stretching rate (c). Fig. 3 is sketched for ($f'(\eta)$) with variation in (β). Velocity ($f'(\eta)$) decays for higher values of (β). Fig. 4 captures the effect of (β_0) on velocity. For larger values of (β_0), the velocity field decreases. Fig. 5 illustrates the influence of the Hartmann number (Ha) on velocity. Velocity field ($f'(\eta)$) drops for higher values of (Ha). Physically, the Hartmann number associated with resistive force (also called the Lorentz force), and as a result, when Hartmann number increases, velocity decays.

Figs. 6–10 demonstrate the influence of the different parameters on the temperature field. Fig. 6 shows the effect of the thermal radiation parameter (Tr) on the temperature ($\theta(\eta)$). Clearly, ($\theta(\eta)$) is

**Fig. 2.** $f'(\eta)$ via We .**Fig. 5.** $f'(\eta)$ via Ha .**Fig. 3.** $f'(\eta)$ via β .**Fig. 6.** $\theta(\eta)$ via T_r .**Fig. 4.** $f'(\eta)$ via β_0 .**Fig. 7.** $\theta(\eta)$ via Pr .

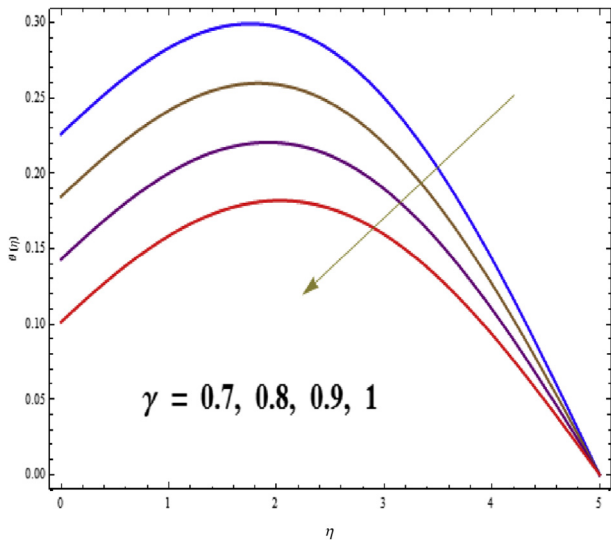
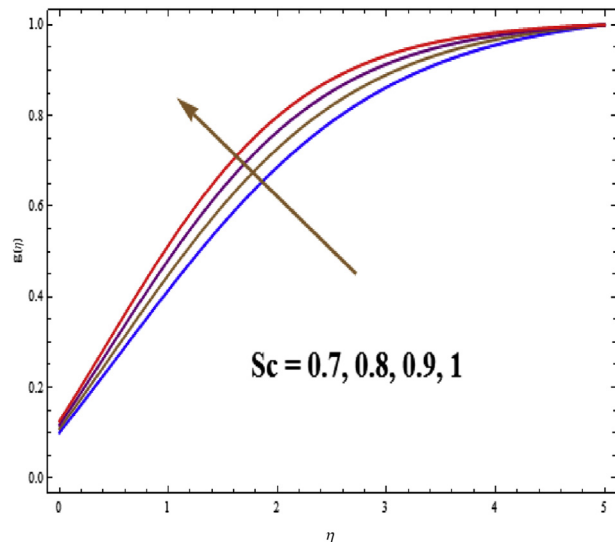
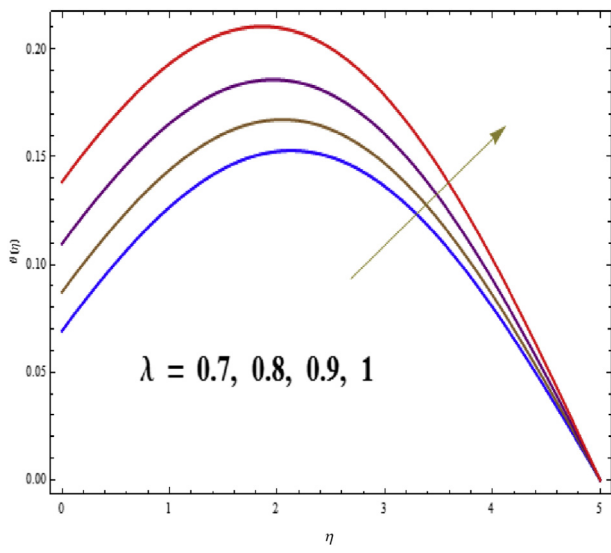
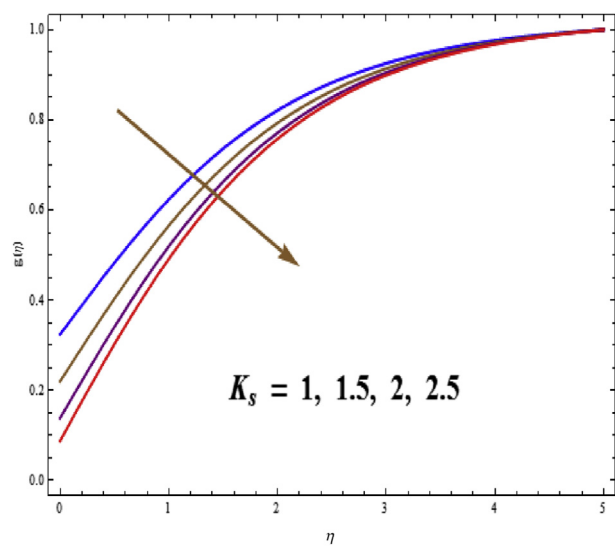
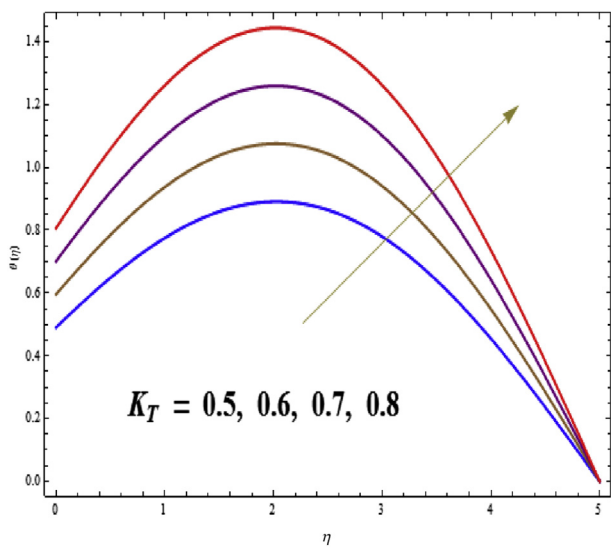
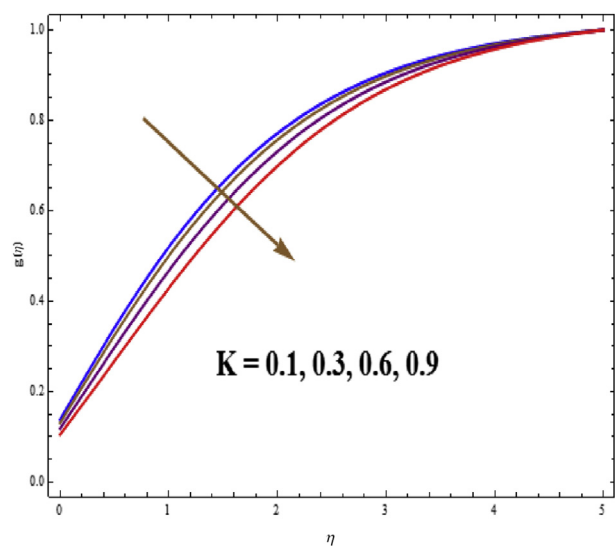
**Fig. 8.** $\theta(\eta)$ via γ .**Fig. 11.** $g(\eta)$ via Sc .**Fig. 9.** $\theta(\eta)$ via λ .**Fig. 12.** $g(\eta)$ via K_s .**Fig. 10.** $\theta(\eta)$ via K_T .**Fig. 13.** $g(\eta)$ via K .

Table 1
Numerical simulation for (C_{fx}).

n	We	Ha	β	β_0	$C_{fx}Re_x^{0.5}$
1.0	0.7	0.4	0.2	0.8	2.88135
1.5					1.56283
2.0	0.7				1.18635
	0.8				1.08483
	0.9				0.99644
0.7	0.4				1.18635
	0.7				1.24094
	0.9				1.26588
0.4	0.2				1.18635
	0.3				1.20764
	0.4				1.22561
0.2	0.8				1.18635
	0.9				1.20046
	1.0				1.21294

Table 2
Numerical simulation for Nu_x .

T_r	Pr	K_T	$Nu_xRe_x^{-0.5}$
0.3	0.2	0.7	-0.137838
0.4			-0.148441
0.5			-0.148443
0.3	0.2		-0.137838
	0.3		-0.137838
	0.4		-0.137838
0.2	0.2	0.7	-0.137838
		0.8	-0.157530
		0.9	-0.177221

an increasing function of (T_r). The characteristic of ($\theta(\eta)$) with variation (Pr) is plotted in Fig. 7. It should be noticed that velocity decays for larger estimation of (Pr). Fig. 8 depicts the influence of (γ) on ($\theta(\eta)$). For higher estimations of (γ), the temperature decreases. Fig. 9 reveals the effect of the heat generation variable (λ) on the temperature ($\theta(\eta)$). Here, temperature rises via (λ). The influence of (K_T) on the temperature is portrayed in Fig. 10. It should be noticed that temperature is an increasing function of (K_T).

Figs. 11–13 are plotted to show the behavior of the concentration ($(g(\eta))$) with variation in the homogeneous variable (K), heterogeneous variable (K_s), and Schmidt number (Sc). Fig. 11 shows the influence of (Sc) on ($(g(\eta))$). Clearly, ($(g(\eta))$) is an increasing function of (Sc), because (Sc) is the ratio of viscosity to mass diffusivity. Therefore, for larger values of (Sc), the viscosity diffusivity is enhanced, which is responsible for the enhancement of ($(g(\eta))$). Fig. 12 illustrates the behavior of ($(g(\eta))$) with variation of (K_s). Concentration drops for larger values of (K_s). The impact of (K) on ($(g(\eta))$) is shown in Fig. 13. Concentration drops via (K). Tables 1 and 2 are constructed to describe the impacts of (n), (We), (Ha), (β), (β_0), (T_r), (Pr), and (K_T) on surface drag force (C_{fx}) and heat transfer rate (Nu_x). Table 1 shows that surface drag force increases for increasing values of (Ha), (β), and (β_0), whereas it decreases with increasing values of (n) and (We). Table 2 shows that heat transfer rate enhanced with (T_r) and (K_T).

5. Concluding remarks

Here, we point out the effects of heat generation, thermal radiation, and chemical reaction (homogeneous–heterogeneous reaction) on flow of Cross fluid in non-Darcy–Forchheimer medium. Major points are listed below:

- Velocity field ($f'(\eta)$) boosts via (We), whereas it reduces with (Ha), (β), and (β_0).

- Temperature field ($\theta(\eta)$) enhanced through (T_r), and (K_T) however decreases with (Pr) and (γ).
- Concentration field ($g(\eta)$) is an increasing function of (Sc) and decays through (K_s) and (K).
- Surface drag force (C_{fx}) increased for larger values of (Ha), (β), and (β_0), whereas it reduces by (n) and (We).
- Temperature gradient boosts via (T_r) and (K_T).

Conflict of interest

There is no conflict of interest among authors.

References

- [1] M.M. Cross, Rheology of non-Newtonian fluids: a new flow equation for pseudoplastic systems, *J. Colloid Sci.* 20 (1965) 417–437.
- [2] T. Hayat, S. Ahmad, M.I. Khan, A. Alsaedi, Simulation of ferromagnetic nanomaterial flow of Maxwell fluid, *Results Phys.* 8 (2018) 34–40.
- [3] M.J. Babu, N. Sandeep, UCM flow across a melting surface in the presence of double stratification and cross-diffusion effects, *J. Mol. Liq.* 232 (2017) 27–35.
- [4] M.I. Khan, T. Hayat, M.I. Khan, A. Alsaedi, Activation energy impact in nonlinear radiative stagnation point flow of Cross fluid, *Int. Commun. Heat Mass Transf.* 91 (2018) 216–224.
- [5] T. Hayat, S. Ahmad, M.I. Khan, A. Alsaedi, Exploring magnetic dipole contribution on radiative flow of ferromagnetic Williamson fluid, *Results Phys.* 8 (2018) 545–551.
- [6] M.I. Khan, M. Waqas, T. Hayat, A. Alsaedi, Magneto-hydrodynamical numerical simulation of heat transfer in MHD stagnation point flow of Cross fluid model towards a stretched surface, *Phys. Chem. Liq.* (2017), <https://doi.org/10.1080/00319104.2017.1367791>.
- [7] I.L. Animasaun, C.S.K. Raju, N. Sandeep, Unequal diffusivities case of homogeneous–heterogeneous reactions within viscoelastic fluid flow in the presence of induced magnetic-field and nonlinear thermal radiation, *Alex. Eng. J.* 55 (2016) 1595–1606.
- [8] S. Qayyum, M.I. Khan, T. Hayat, A. Alsaedi, A framework for nonlinear thermal radiation and homogeneous–heterogeneous reactions flow based on silver-water and copper–water nanoparticles: a numerical model for probable error, *Results Phys.* 7 (2017) 1907–1914.
- [9] M.I. Khan, M. Waqas, T. Hayat, A. Alsaedi, M.I. Khan, Significance of nonlinear radiation in mixed convection flow of magneto Walter-B nanoliquid, *Int. J. Hydrogen Energy* 42 (2017) 26408–26416.
- [10] R. Kumar, S. Sood, M. Sheikholeslami, S.A. Shehzad, Nonlinear thermal radiation and cubic autocatalysis chemical reaction effects on the flow of stretched nanofluid under rotational oscillations, *J. Colloid Sci.* 505 (2017) 253–265.
- [11] M.I. Khan, M. Waqas, T. Hayat, M.I. Khan, A. Alsaedi, Numerical simulation of nonlinear thermal radiation and homogeneous–heterogeneous reactions in convective flow by a variable thickened surface, *J. Mol. Liq.* 246 (2017) 259–267.
- [12] T. Hayat, M.I. Khan, M. Farooq, T. Yasmeen, A. Alsaedi, Stagnation point flow with Cattaneo–Christov heat flux and homogeneous–heterogeneous reactions, *J. Mol. Liq.* 220 (2016) 49–55.
- [13] B.C. Prasannakumara, B.J. Gireesha, M.R. Krishnamurthy, K.G. Kumar, MHD flow and nonlinear radiative heat transfer of Sisko nanofluid over a nonlinear stretching sheet, *Inform. Med. Unlocked* 9 (2017) 123–132.
- [14] G.T. Thammanina, K.G. Kumar, B.J. Gireesha, G.K. Ramesh, B.C. Prasannakumara, Three dimensional MHD flow of couple stress Casson fluid past an unsteady stretching surface with chemical reaction, *Results Phys.* 7 (2017) 4104–4110.
- [15] K.G. Kumar, B.J. Gireesha, B.C. Prasannakumara, G.K. Ramesh, O.D. Makinde, Phenomenon of radiation and viscous dissipation on Casson nanoliquid flow past a moving melting surface, *Diffus. Found.* 11 (2017) 33–42.
- [16] K.G. Kumar, B.J. Gireesha, B.C. Prasannakumara, O.D. Makinde, Impact of chemical reaction on Marangoni boundary layer flow of a Casson nano liquid in the presence of uniform heat source sink, *Diffus. Found.* 11 (2017) 22–32.
- [17] K.G. Kumar, B.J. Gireesha, M.R. Krishnamurthy, B.C. Prasannakumara, Impact of convective condition on Marangoni convection flow and heat transfer in Casson nanofluid with uniform heat source sink, *J. Nanofluids* 7 (1) (2017) 108–114.
- [18] T. Hayat, M.I. Khan, M. Farooq, A. Alsaedi, M. Waqas, T. Yasmeen, Impact of Cattaneo–Christov heat flux model in flow of variable thermal conductivity fluid over a variable thickened surface, *Int. J. Heat Mass Transf.* 99 (2016) 702–710.
- [19] M. Ramzan, J.D. Chung, N. Ullah, Radiative magnetohydrodynamic nanofluid flow due to gyrotactic microorganisms with chemical reaction and non-linear thermal radiation, *Int. J. Mech. Sci.* 130 (2017) 31–40.
- [20] O.D. Makinde, I.L. Animasaun, Thermophoresis and Brownian motion effects on MHD bioconvection of nanofluid with nonlinear thermal radiation and

- quartic chemical reaction past an upper horizontal surface of a paraboloid of revolution, *J. Mol. Liq.* 221 (2016) 733–743.
- [21] P. Forchheimer, Wasserbewegung durch Boden, *Z. Ver. D. Ing.* 45 (1901) 1781.
- [22] T. Hayat, S. Ahmad, M.I. Khan, A. Alsaedi, Non-Darcy Forchheimer flow of ferromagnetic second grade fluid, *Results Phys.* 7 (2017) 3419–3424.
- [23] T. Hayat, Z. Hussain, B. Ahmed, A. Alsaedi, Base fluids with CNTs as nanoparticles through non-Darcy porous medium in convectively heated flow: a comparative study, *Adv. Powder Tech.* 28 (2017) 1855–1865.
- [24] T. Hayat, F. Shah, A. Alsaedi, M.I. Khan, Development of homogeneous/heterogeneous reaction in flow based through non-Darcy Forchheimer medium, *J. Theor. Comput. Chem.* 16 (2017), 1750045.
- [25] M.I. Khan, M. Waqas, T. Hayat, A. Alsaedi, A comparative study of Casson fluid with homogeneous-heterogeneous reactions, *J. Colloid Sci.* 498 (2017) 85–90.
- [26] T. Hayat, S. Ullah, M.I. Khan, A. Alsaedi, On framing potential features of SWCNTs and MWCNTs in mixed convective flow, *Results Phys.* 8 (2018) 357–364.
- [27] T. Hayat, M.I. Khan, M. Tamoor, M. Waqas, A. Alsaedi, Numerical simulation of heat transfer in MHD stagnation point flow of Cross fluid model towards a stretched surface, *Res. Phys.* 7 (2017) 1824–1827.
- [28] T. Hayat, M.I. Khan, S. Qayyum, A. Alsaedi, Modern developments about statistical declaration and probable error for skin friction and Nusselt number with copper and silver nanoparticles, *Chinese J. Phys.* 55 (2017) 2501–2513.